


Measurement of a charge qubit using a single-electron transistor based on a triple quantum dotA. V. Tsukanov *Valiev Institute of Physics and Technology of Russian Academy of Sciences, 117218 Moscow, Russia*

(Received 23 April 2019; published 4 December 2019)

A scheme for determining an arbitrary pure state of a charge qubit by measuring a steady-state current through a single-electron transistor is proposed. In order to increase the sensitivity of the transistor its operating part consists of three quantum dots, the energy levels of which form a symmetrical configuration. Such a choice makes it possible to realize high-precision measurements in a nonresonant steady-state regime when a maximum distance of the qubit from this structure is several hundreds of nanometers. Time-dependent populations of the structure states are obtained; a current and a measurement contrast are calculated as functions of system geometric parameters and the optimal values of these parameters are found.

DOI: [10.1103/PhysRevA.100.062305](https://doi.org/10.1103/PhysRevA.100.062305)**I. INTRODUCTION**

A necessary condition for a quantum system to be a potential candidate for a quantum bit (qubit) is the possibility of its scaling, since only a full-scale quantum computer consisting of a large number of qubits will surpass up-to-date classical supercomputers. Ones of the most suitable systems for this purpose are that of solid-state nanostructures. They can be manufactured using micro- and nanotechnologies of the modern semiconductor industry which have a great potential for further development. Nanostructures formed on the basis of quantum dots (QDs) are of particular interest [1]. Especially, a structure consisting of two QDs [double QD (DQD)] and containing one electron is often proposed as a solid-state scalable charge qubit [2,3]. Orbital states of the electron localized in different QDs serve as the logical states of such a qubit. Experiments clearly demonstrate the principles of the coherent control of a single-electron DQD dynamics by means of the dc voltage applied to metal gates located on a dielectric layer directly above the structure or near it [4–6].

An ability to measure the qubit states reliably is also one of the main requirements for the implementation of quantum algorithms. Usually the charge qubit state is measured by use of a single-electron transistor (SET)—a quantum detector operating in the Coulomb blockade regime [7]. The SET sensing element (an island), the susceptibility of which to the external field sets the measurement precision, is ordinarily represented by a QD or a metal particle. Its electronic energy spectrum has a high discreteness. The charge carriers are transferred from the source to the SET central region where the QD is located and further move into the drain due to electron tunneling. In this case, the energy of the Coulomb interaction of the QD electrons is so large that the injection of the second electron shifts the energy of the transport level above the source Fermi energy. This immediately leads to a drop of the current through the QD and thus only one electron can be inside the QD. The name of this device reflects that circumstance. The field created by the qubit electron located in the vicinity of the SET also shifts the energy of the QD transport level due to the Stark effect. Here, the magnitude of

the SET current depends on the spatial position of the electron in the DQD. Consequently, by measuring the current through the detector it is possible to determine the qubit state. The charge sensitivity of the SET depends on the ratio of zero-frequency noise to the differential conductance according to the general formalism of the quantum measurement theory [8]. Consequently, the optimized operation condition of a SET is the maximal conductance-to-noise ratio. SET can operate near the quantum limit: Amplification can be accomplished with a back action close to that required by the uncertainty principle. Its charge sensitivity is ultimately limited to about $10^{-6} e/\text{Hz}^{1/2}$ [9] or even $10^{-7} e/\text{Hz}^{1/2}$ [10] by the shot noise in the source-drain current. In practice, the sensitivity limit for the SET depends on the temperature, noise intensity, and island or gate geometry. Despite considerable efforts, the shot-noise limit has yet to be reached.

In this paper we propose an alternative SET design in order to improve its measuring properties. We replace a single QD with a linear structure—a “molecule” of three tunnel-connected single-level QDs. As will be shown, in this case the current is more sensitive to the electric field change associated with the electron movement inside the qubit. For this purpose one should use a nonresonant tunneling regime shifting the energy level of the central QD by an amount significantly exceeding the tunneling energy, while the energy levels of the outer QDs stay equal. This makes it possible to carry out measurements in the regime when the SET tunneling channel is open only for one logical qubit state.

Time-dependent populations of the states are obtained by numerical simulation of electron dynamics in an open structure. The current through the SET in a steady-state regime demonstrates stability with respect to fluctuations of some quantities, which usually lead to a breakdown of the electronic coherent transport in a closed structure. In order to improve the quality of measurements, which are based on the fact that the interaction energy between the electrons of the SET and the qubit depends on the state of the latter, a planar structure of the measuring chip with a specified configuration of the QDs was developed. Optimization of the SET measuring properties (sensitivity, contrast, current) is possible over each system

parameter. We study the behavior of these characteristics varying the geometry of the chip and the QD energy levels. One of the interesting features inherent in the measurements with use of the proposed chip is the possibility of compensating for the technological asymmetry by creating a controlled asymmetry of the energy levels of the SET QDs.

II. MODEL OF THE CHARGE QUBIT COUPLED TO THE SINGLE-ELECTRON TRANSISTOR BY THE ELECTROSTATIC INTERACTION

We use a charge qubit model based on a single-electron QD consisting of two QDs A and B , which for simplicity are considered identical [2]. Let us assume the presence of two ground orbital states $|A\rangle$ and $|B\rangle$ of the electron with wave functions $\psi_A(\mathbf{r}) = \langle \mathbf{r} | A \rangle$ and $\psi_B(\mathbf{r}) = \langle \mathbf{r} | B \rangle$ localized in the QD A and the QD B , respectively. If the quantum-state energy of an electron in the isolated QD is significantly larger than the matrix element V_0 of tunneling between the ground states of neighboring QDs, then one can apply the tight-binding approximation for the Hamiltonian of an electron being in one of these states (or their superposition):

$$H_{\text{qubit}} = \varepsilon_A |A\rangle \langle A| + \varepsilon_B |B\rangle \langle B| - V_0(|A\rangle \langle B| + |B\rangle \langle A|), \quad (1)$$

where ε_A and ε_B are energies of the ground single-electron states $|A\rangle$ and $|B\rangle$ of the isolated QDs. The Hamiltonian parameters smoothly depend on time. Let us choose the ground states $|A\rangle$ and $|B\rangle$ of the electron in the QD A and the QD B , respectively, as the qubit logical states 0 and 1. An electron-state vector $|\Psi(t)\rangle$ can be represented as

$$|\Psi(t)\rangle = c_A(t)|A\rangle + c_B(t)|B\rangle. \quad (2)$$

Quantum operations leading to the required set of probability amplitudes are realized under external electric fields that affect the parameters of the Hamiltonian (1). The qubit state is measured when the control field is turned off, $\varepsilon_{A,B} = \text{const.}$ and $V_0 = 0$.

Now consider a quasi-one-dimensional SET nanostructure, consisting of two metal contacts, which are electron reservoirs (source S and drain D), and a chain of three QDs (L , C , and R). Due to a configuration of the Fermi levels $\varepsilon_{S(D)}$ of the contacts and the QD levels (Fig. 1) the movement of electrons

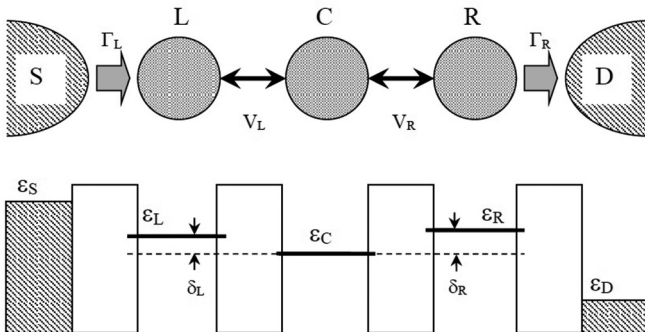


FIG. 1. Top: a SET scheme with a central part represented by three tunnel-coupled QDs. Bottom: the SET potential profile and energy levels of QDs. The dotted line indicates the energy of the central QD state $|C\rangle$.

through the structure from left to right is possible. To describe the process of the electron injection from the source into the left QD L and from the right QD R to the drain, we use a realistic and conventional model of incoherent tunneling [11]. Inside the nanostructure the electron tunnels between the QDs in a coherent manner.

We assume the presence of bound states $|L\rangle$ in the left QD, $|R\rangle$ in the right QD, and $|C\rangle$ in the central QD with energies ε_L , ε_R , and ε_C , respectively. It is convenient to introduce energy differences (detunings) between the ground states of the outer QDs and one of the central QD, $\delta_L = \varepsilon_L - \varepsilon_C$ and $\delta_R = \varepsilon_R - \varepsilon_C$. They are determined by a shape and a chemical composition of the QDs during a fabrication and can be controlled using external electrical gates [4–10]. The states $|L(R)\rangle$ and the state $|C\rangle$ are interconnected by single-electron tunneling $V_{L(R)}$. For shallow QDs, the second electron injection leads to pushing of the level into a continuous spectrum and, as a result, to the electron transport termination. Therefore, two-particle effects are restricted to the charge configurations in which electrons occupy levels in different QDs. The energy of the Coulomb interaction of the two electrons in the SET state $|j, k\rangle$ ($j, k = L, C, R$) is denoted by $U_{j,k}$. The Hamiltonian of the three-QD linear structure is

$$H_{\text{SET}} = H_0 + H_V + H_{\text{coul}}, \quad (3)$$

$$H_0 = \varepsilon_L |L\rangle \langle L| + \varepsilon_R |R\rangle \langle R| + \varepsilon_C |C\rangle \langle C|, \quad (4)$$

$$H_V = -V_L(|C\rangle \langle L| + |L\rangle \langle C|) - V_R(|C\rangle \langle R| + |R\rangle \langle C|), \quad (5)$$

$$H_{\text{coul}} = U_{L,R}|L, R\rangle \langle L, R| + U_{L,C}|L, C\rangle \langle L, C| + U_{R,C}|R, C\rangle \langle R, C|. \quad (6)$$

Choosing the energy ε_C of the state $|C\rangle$ as a reference, one can rewrite the Hamiltonian (4) in the form $H_0 = \delta_L |L\rangle \langle L| + \delta_R |R\rangle \langle R|$.

The Coulomb interaction of the charge qubit electron with electrons tunneling through the SET results in shifts of the system-state energies:

$$H_{\text{qubit-SET}} = W_{A,L}|A, L\rangle \langle A, L| + W_{A,C}|A, C\rangle \langle A, C| + W_{A,R}|A, R\rangle \langle A, R| + W_{B,L}|B, L\rangle \langle B, L| + W_{B,C}|B, C\rangle \langle B, C| + W_{B,R}|B, R\rangle \langle B, R|, \quad (7)$$

where $W_{i,j}$ is a pair interaction of the qubit electron in the state $|i\rangle$ ($i = A, B$) with the SET one in the state $|j\rangle$ ($j = L, C, R$).

In order to study the evolution of the system state, represented by the density matrix ρ , we use the Lindblad equation, which includes dissipative components:

$$\begin{aligned} \frac{d\rho}{dt} = & -i[H_{\text{qubit}} + H_{\text{SET}} + H_{\text{qubit-SET}}, \rho] + \Gamma_L D(|L\rangle \langle vac_L|) \\ & + \Gamma_R D(|vac_R\rangle \langle R|) + \gamma_{\text{rel},L} D(|C\rangle \langle L|) + \gamma_{\text{rel},R} D(|C\rangle \langle R|) \\ & + \gamma_{\text{deph},L} D(|L\rangle \langle L| - |C\rangle \langle C|) + \gamma_{\text{deph},R} D(|R\rangle \langle R| \\ & - |C\rangle \langle C|) + \gamma_{\text{deph},q} D(|A\rangle \langle A| - |B\rangle \langle B|). \end{aligned} \quad (8)$$

Such approach makes it possible to consider the open structure in the current regime. The electrons enter the left QD from the source S at the rate Γ_L (provided that the state $|L\rangle$ is

not populated) and leave the right QD to the drain D at the rate Γ_R . These processes are irreversible and are simulated by Lindblad operators $D(O) = O\rho O^\dagger - [O^\dagger O, \rho]/2$. The state $|vac_{L(R)}\rangle$ describes the QD $L(R)$ without electrons.

Similarly, dissipative processes that affect the dynamics of charge carriers, i.e., relaxation and dephasing, are introduced. During the measurement, the logical states $|A\rangle$ and $|B\rangle$ of the qubit are isolated from each other, and electron relaxation is suppressed. However, coupling of the DQD to thermal phonons of a crystal lattice causes stochastic fluctuations of the logical states' energies leading to qubit dephasing with the rate $\gamma_{\text{deph},q}$. The geometry of the SET considered is such that the state energies of the outer QDs are about the same, and the state energy of the central QD is less by an amount of $\delta_{L(R)}$ exceeding the tunneling $V_{L(R)}$. Then the electron can relax from the state $|L(R)\rangle$ to the state $|C\rangle$ by emitting a phonon with a frequency $\delta_{L(R)}$. The electron relaxation rate is $\gamma_{\text{rel},L(R)}$ and the relaxation mechanism depends on the transition frequency. In GaAs QDs at frequencies below 1 meV the relaxation is associated with acoustic phonons, but above 10–15 meV it is due to processes of the polaron decay, which is a correlated (entangled) state of the electron and some set of degenerate optical phonon modes [12]. At nonzero temperature T , a reverse process is also possible (incoherent phonon absorption). We consider $T \ll \delta_{L(R)}$ that makes the phonon absorption unlikely. We neglect these processes in Eq. (8). Similar to the qubit, thermal fluctuations of the phonon field cause dephasing of the outer SET states relative to the central one with rates $\gamma_{\text{deph},L}$ and $\gamma_{\text{deph},R}$. Since the rate Γ_L of SET incoherent pumping is much larger than the phonon relaxation and dephasing ones, then level broadening is mainly determined by Γ_L . The dissipation effect on the coherent evolution of the QD qubits prevents the implementation of quantum operations; however, in the steady state it can increase the measurement rate [13].

Equation (8) is integrated over a sufficiently large time interval $t^{\text{SS}} \approx 1/\Gamma_{L(R)}$; after that the system goes into the steady state. We choose the vacuum state $|vac\rangle$ with no electrons in the structure as the SET initial state. The density matrix of the initial state of the ‘‘qubit + SET’’ system has the form $\rho(0) = |vac\rangle\langle vac| \otimes |\Psi\rangle\langle\Psi|$. The final result of the calculations is the population $\tilde{\rho}_{RR}(t)$ of the state $|R\rangle$ of the SET right QD. The matrix $\tilde{\rho}(t) = \text{Tr}_{\text{qubit}}\rho(t)$ is the reduced SET density matrix, which is obtained by taking a partial trace of the matrix $\rho(t)$, being a solution of Eq. (8) with the initial condition mentioned above, over the qubit states. The output current in the steady state,

$$I = 2\pi e\Gamma_R \tilde{\rho}_{RR}^{\text{SS}}/\hbar, \quad (9)$$

is proportional to $\tilde{\rho}_{RR}^{\text{SS}} = \tilde{\rho}_{RR}(t^{\text{SS}})$. As one shall see, it depends on various factors and, first of all, on the qubit state. As measurement units we take the effective atomic units, assuming 1 a.u. = $\text{Ry}^* = m^*\text{Ry}/m_e\epsilon^2$ for energy and 1 a.u. = $a_B^* = a_B m_e \epsilon / m^*$ for length, where $\text{Ry} = 13.6\text{ eV}$ is the Rydberg energy, $a_B = 0.52 \times 10^{-10}\text{ m}$ is the Bohr radius, m_e (m^*) is the free (effective) electron mass, and ϵ is the permittivity of the semiconductor. For GaAs ($\epsilon = 12$ and $m^* = 0.067m_e$) one has $\text{Ry}^* = 6\text{ meV}$ and $a_B^* = 10\text{ nm}$.

The principle of measuring of the charge qubit state using the SET is based on the fact that each state (2) corresponds to a certain magnitude of the steady-state current flowing through the SET. Optimization of the measurement procedure is to choose the relative position of the qubit and the SET, at which the current difference for the basis qubit states is maximum. Below we represent the results of the SET and qubit dynamics simulation, illustrating features and benefits of this scheme.

III. MEASUREMENT OF AN ARBITRARY PURE CHARGE QUBIT STATE

The interaction of the qubit and the SET leads to the entanglement of their quantum degrees of freedom. The density matrix of the system in the steady state is diagonal:

$$\rho^{\text{SS}} = \tilde{\rho}^{\text{SS}}(A) \otimes \rho'_{AA} |A\rangle\langle A| + \tilde{\rho}^{\text{SS}}(B) \otimes \rho'_{BB} |B\rangle\langle B|, \quad (10)$$

where ρ'_{AA} and ρ'_{BB} are the populations of the basis qubit states. Taking the trace over the qubit states gives the reduced density matrix of the SET:

$$\tilde{\rho}^{\text{SS}} = \text{Tr}_{\text{qubit}}\rho^{\text{SS}} = \tilde{\rho}^{\text{SS}}(A)\rho'_{AA} + \tilde{\rho}^{\text{SS}}(B)\rho'_{BB}. \quad (11)$$

If the qubit at the start of measurements is in an arbitrary pure state $|\Psi\rangle = c_A|A\rangle + c_B|B\rangle$ then, provided that the relaxation of the qubit can be neglected and $\rho'_{AA} = |c_A|^2$ and $\rho'_{BB} = |c_B|^2$ in Eq. (11), the expression (9) for a stationary current through the SET acquires a simple form:

$$I(\Psi) = |c_A|^2 I_A + (1 - |c_A|^2) I_B, \quad (12)$$

where $I_k = 2\pi e\Gamma_R \tilde{\rho}_{RR}^{\text{SS}}(k)/\hbar$ is the current associated with the qubit basis state $|k\rangle$ ($k = A, B$). Thus, the absolute values of the probability amplitudes are

$$|c_A| = \sqrt{\frac{I(\Psi) - I_B}{I_A - I_B}}, \quad |c_B| = \sqrt{1 - |c_A|^2}. \quad (13)$$

In order to determine the phase difference $\Delta\phi = \arg c_A - \arg c_B$ of the qubit basis states, it is necessary to apply the Hadamard gate $\text{Had} = (|A\rangle\langle A| + |A\rangle\langle B| + |B\rangle\langle A| - |B\rangle\langle B|)/\sqrt{2}$ to the initial state, that converts the initial state phase into amplitude, and to measure the current $I(\Psi_H)$ of the qubit being in the state $|\Psi_H\rangle = \text{Had}|\Psi\rangle$. It is easy to show that the phase difference is calculated by

$$\Delta\phi = \arccos \left\{ \frac{1}{2} \frac{[2I(\Psi_H) - I_A - I_B][I_A - I_B]}{\sqrt{[I(\Psi) - I_B][I_A - I(\Psi)]}} \right\}. \quad (14)$$

Therefore, to determine the qubit state three operations are sufficient: two measurements of the current through the SET and the Hadamard gate applied to the qubit.

An important characteristic of a measuring device is the ability to distinguish between two states of a measured object that are close in physical properties. The derivative $dI/d|c_A|$ characterizes the possibility of experimental resolution of two qubit states with close probability amplitude distributions. For example, if the error of indication of the ammeter is δI , the qubit states from the range $\delta|c_A| \approx \delta I/[dI/d|c_A|]$ cannot be resolved. Therefore, at some fixed instrumental error (here δI) this derivative should be sufficiently large to achieve the measurement accuracy required by a given quantum algorithm

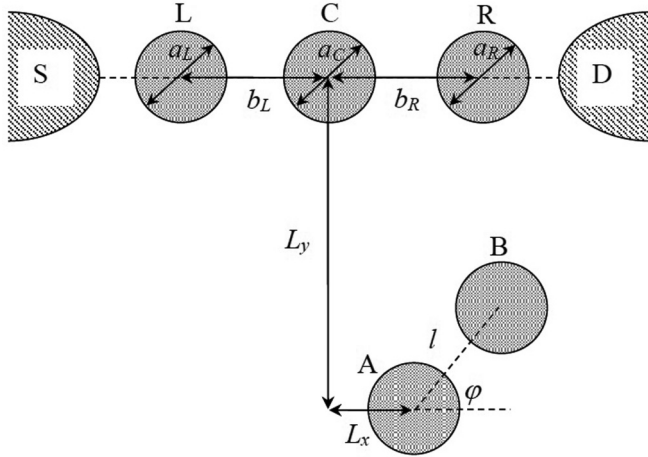


FIG. 2. A scheme of the measuring chip, consisting of the SET (top) and the charge DQD qubit (bottom); see text.

or state tomography process. Quantitatively this property is associated with the measuring contrast (visibility):

$$C_I = |(I_A - I_B)/(I_A + I_B)|, \quad (15)$$

since $dI/d|c_A| = 2C_I(I_A + I_B)|c_A|$. Hence, in order to optimize the detection procedure with use of the SET it is necessary to find system parameters at which C_I is maximum. Below we analyze the geometric parameters and point out the conditions that ensure a high reliability of measuring the qubit state.

Consider the scheme of the measuring chip shown in Fig. 2. We place the origin at the center of the QD C with the X axis passing through the centers of the QDs L , C , and R , and the Y axis is directed vertically downwards. The center of the qubit QD A is located at the position with coordinates (L_x, L_y) , and the distance between the centers of the QDs A and B (the “qubit length”) is l . The characteristic size (width) of the QD k is equal to a_k , the distance between the centers of the QDs C and L (R) is b_L (b_R), and the angle between the qubit axis and the SET axis is φ . The energies of the Coulomb interaction of two electrons in the QDs j and k with known wave functions in Hamiltonians (6) and (7) are calculated by the formula

$$U(W)_{j,k} = 2 \iint \frac{|\psi_j(\mathbf{r}_1)|^2 |\psi_k(\mathbf{r}_2)|^2 d\mathbf{r}_1 d\mathbf{r}_2}{|\mathbf{r}_1 - \mathbf{r}_2|}. \quad (16)$$

If the electron density in the QD ground state is assumed to be concentrated in its central area, then one can consider electrons as point charges. In this case, the energies of the pair interaction are $U(W)_{j,k} = 2/r_{j,k}$, where $r_{j,k}$ is the distance *between the centers* of the QDs j and k . To validate the charge point approximation the Coulomb interaction energies U and W have been computed (a) according to the exact formula (16) by Monte Carlo simulation and (b) within the point charge framework. The results obtained for two-dimensional squarelike QDs have demonstrated that the approximation works with very good accuracy if the distance $r_{j,k}$ is twice as large or larger than their typical size. The exchange and cotunneling energies have been also numerically estimated but their values are three orders of magnitude smaller than single-electron tunneling energy. Thus, one can safely neglect them

in this study. To estimate the tunneling energies in expression (5) we use the approximation

$$V(b) = V(b_1) \exp \left\{ - \left[\ln \frac{V(b_1)}{V(b_2)} \right] \frac{b - b_1}{b_2 - b_1} \right\}, \quad (17)$$

constructed from two known values of $V(b_1)$ and $V(b_2)$, which is found in the framework of the microscopic model of two-dimensional QDs [14]. Here b is the distance between the centers of neighboring QDs, which is the sum of the barrier width and a half of the sum of the QD widths. The magnitudes describing the dissipative effects (including tunnel coupling between the QDs and the reservoirs) are considered as phenomenological parameters that take values from a certain interval. The arrangement of the chip functional elements shown in Fig. 2 makes it possible to realize the measurement in the nonresonant tunneling regime, which, as we see further, turns out to be more advantageous than the convenient resonant scheme.

The phenomenological parameters of the system are extracted from experimental works in which such structures have been studied. The current magnitude I measured at the SET output is usually several nanoamperes, which gives an estimate of $\Gamma_{L,R} \approx 10^{-4}$ in effective atomic units. Experiments are carried out in the temperature range $T = 0.1 - 1$ K, which corresponds to the energy interval $10^{-3} - 10^{-2}$. The times of electronic relaxation and dephasing, as mentioned above, depend on the geometry and the material of the nanostructure. We assume that for all dissipative processes the characteristic times are hundreds of picoseconds, and $\gamma_{\text{deph},q}$, $\gamma_{\text{rel},L(R)}$ as well as $\gamma_{\text{deph},L(R)}$ turn out to be about $10^{-4} - 10^{-3}$. In what follows we set $\Gamma_{L,R} = 8 \times 10^{-5}$, $\gamma_{\text{rel},L(R)} = \gamma_{\text{deph},L(R)} = \gamma_{\text{deph},q} = 16 \times 10^{-5}$, and use these parameters throughout the paper. These estimates are in good agreement with the results of the theoretical model and the experimental studies [4–10]. Note that the dissipation rate values used here have not changed significantly during almost two decades. In particular, the reason is concerned with the charge noise caused by the electrostatic gates being rather complex to be filtered out (e.g., by the geometry and material optimization). However, even at these dissipation rates the current actively flows through the SET thus enabling the measurement. Only when the tunneling becomes ineffective does the relaxation localize an electron in the deeper QD C and the current is stopped. Therefore, one should take the tunneling rate V to meet the condition $V_{L(R)} \gg \max(\gamma_k)$. The measurement technique for single-electron DQDs was described and applied in Ref. [6]. There the GaAs/AlGaAs-based heterostructure contained a two-dimensional electron gas with a density of $2 \times 10^{11} \text{ cm}^{-2}$ and a mobility of $2 \times 10^5 \text{ cm}^2/\text{s V}$ at a depth of ~ 100 nm from the surface. Twelve metal (Ti/Au) Schottky electrodes (gates), deposited on the surface of the chip, formed the DQD qubit as well as a highly sensitive detector determining the amount of electrons with a measuring current of 1 nA. The variation of voltages led to the injection (ejection) of electrons into (from) the DQD that changed the current through the detector. In this setup the measuring current flows through the quantum point contact, i.e., a quasi-one-dimensional constriction formed in two-dimensional electron gas by long electrodes. Two contacts were formed at 500 nm from the left and right QDs of the charge DQD qubit. This geometry of

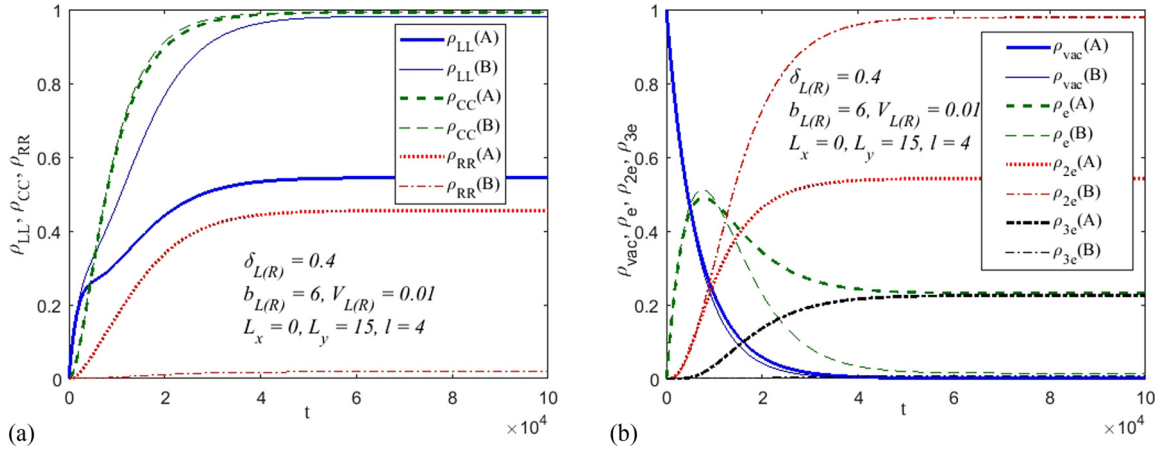


FIG. 3. Populations of the QDs L , C , and R (a) and number of electrons (b) in the SET vs time for two logical states of the qubit associated with an electron in the QDs A or B . (The values are given in effective atomic units for GaAs; see text.)

measurement devices has enabled us to independently probe the electron populations in both QDs. Since the size-quantization energy of this DQD was 1 meV, the qubit dynamics in the single-electron regime was described by the Hamiltonian (1) with good accuracy. The authors estimated a qubit dephasing time of more than 400 ps at a temperature of 135 mK.

The population of the QD R (and, therefore, the current through the SET) depends on a large number of parameters included in Eq. (8), which, in turn, depend on the chip geometry and material. At sufficiently small distance between the QDs L , C , and R , the size and the shape of which are nearly the same, $\delta_{L(R)} \ll V_{L(R)}$ and tunnel coupling between the QDs turns out to be *resonant*. This results in strong hybridization of the individual QD states and in the creation of a triplet of states that are delocalized over the structure. According to the tight-binding model of the electron tunneling in the QD chain, the width of the hybridized state subband is $V_{L(R)}$ if the energies of all QDs are equal or close to each other. Thus the current through the QD chain can flow unless the state energy difference of neighboring QDs becomes substantially larger than $V_{L(R)}$. In this case, the electron transport through the SET turns out to be stable with respect to small Stark energy shifts of the QDs caused by the qubit. This naturally leads to a sharp decrease of the contrast, if the qubit is located at a significant distance from the SET. To increase the sensitivity of the device, it is possible to switch to the *nonresonant* tunneling regime by detuning the state energy of the central QD from the state energies of the outer QDs by an amount essentially exceeding tunneling: $\delta_{L(R)} \gg V_{L(R)}$. In the three-QD chain considered here the off-resonant tunneling regime is possible due to the structure symmetry relative to the central QD. In the off-resonant case the width of the hybridized states is $V_{L(R)}^2/|\delta_{L(R)}|$. Then the current flows through the SET only if the symmetry condition $\delta_L = \delta_R$ is met, and even small deviations of the order of $V_{L(R)}^2/|\delta_{L(R)}| \ll V_{L(R)}$ from the symmetry of the detunings cause the current to be blocked. Thus our approach based on the off-resonant regime for triple QD structure, compared to the resonant one, provides more sensitive detection of energy shifts caused by the qubit electron position. In this regime the outer QDs L and

R are coupled by nonresonant tunneling. The C_l optimization can be carried out either by increasing the detuning, or by reducing the tunneling energy. However, one should remember that the condition $C_l \approx 1$ alone does not guarantee reliable measurement. The steady-state current must be large itself. A typical dependence of the diagonal elements of the SET density matrix on time for two qubit basis states, illustrating the system transition to the steady-state nonresonant regime, is shown in Fig. 3(a). The average number of electrons in the SET (vacuum, one-, two-, and three-electron configurations) is presented in Fig. 3(b).

First of all, note that the SET evolution has a pronounced dissipative character: There are no oscillations inherent in the coherent electron dynamics. The system goes into a steady state at $t^{SS} \approx 1/\Gamma_{L(R)}$. Since at $L_x = 0$ the qubit QD A is equidistant from the QDs L and R of the SET, then $W_{L,A} = W_{R,A}$ and the equality of the detunings is preserved for the basis state $|A\rangle$ at any L_y , ensuring a large current. On the other hand, couplings the electron of the QD B to ones of the QD L and R is different, creating an imbalance of detunings. If $|W_{R,B} - W_{L,B}| \geq V_{L(R)}^2/|\delta_{L(R)}|$ (i.e., the imbalance is greater than the off-resonant tunneling peak width), then the current drops to zero. As for a distribution of the average population over the particle number in the structure, in the current regime, when the qubit electron is in the state $|A\rangle$, there are 22%–23% of total population for one-electron and three-electron components, and about 55% for a two-electron component. The probability of detecting the SET in a vacuum state tends to zero. For the qubit with an electron in the QD B a two-particle component is 100%. In this case, the first electron entering the QD L from the source passes into the QD C and remains in it as a result of the irreversible relaxation process. The second electron populates QD L and, not being able to go to the already occupied QD C , blocks the flow of electrons to the SET. It should be mentioned that for the parameters used, the off-resonant tunneling rate, $V_{L(R)}^2/|\delta_{L(R)}|$, while much smaller than the resonant tunneling rate $V_{L(R)}$, is still larger than the dephasing rates. Thus, the off-resonant tunneling rate is what sets the sensitivity of the proposed device, and not the dephasing rates.

We investigate the tunneling influence on the SET measuring properties by simultaneously varying the distances

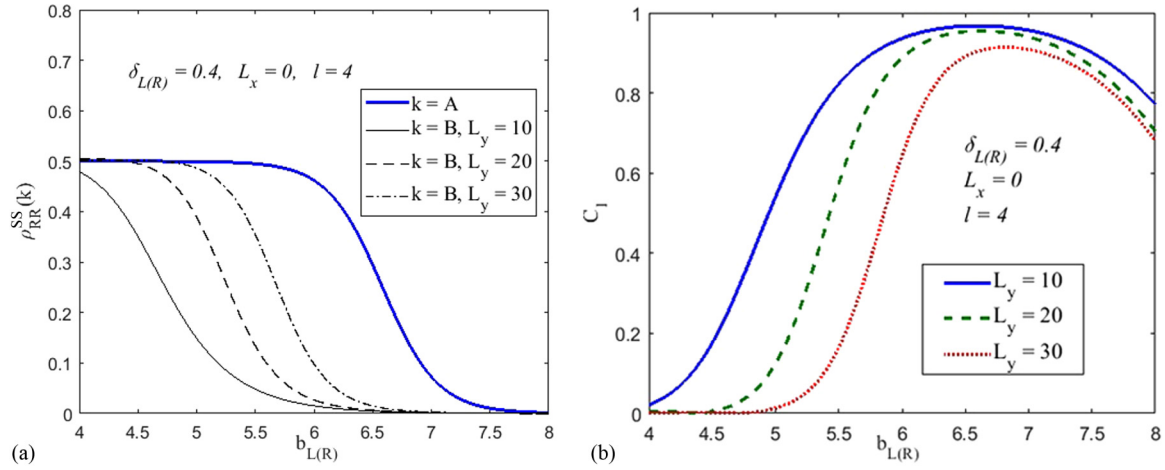


FIG. 4. The population of the QD R of the SET (current strength) for the qubit in states $|A\rangle$ and $|B\rangle$ (a) and the measuring contrast (b) as functions of the distance between the centers of the neighboring QDs in the SET in the steady-state ($t^{SS} = 10^5$) nonresonant regime. (The values are given in effective atomic units for GaAs; see text.)

$b_L = b_R$ between the centers of the QD C and the QDs $L(R)$. The value of $V_{L(R)}$ depends on $b_{L(R)}$ exponentially, which causes a fast monotonous decrease of the current with increasing the thickness of the potential barrier between the QDs. This is due to a suppression of tunnel coupling starting at $b_{L(R)} = 6$ for the qubit in the state $|A\rangle$ and at $b_{L(R)} = 4-4.5$ for the state $|B\rangle$ [Fig. 4(a)]. The curves for a symmetric electronic configuration with $k = A$ practically do not change for different L_y , but for an asymmetric configuration with $k = B$ such an effect exists. One can note that as the ratio l/L_y decreases, the curve $\rho_{RR}^{SS}(B)$ tends to $\rho_{RR}^{SS}(A)$, which causes decreasing of the contrast (more strictly, leads to narrowing the large C_I interval). The latter is directly related to the minimization of the detuning imbalance, which makes it possible to determine the position of an electron in the qubit for large distances L_y .

A decrease in C_I at $b_{L(R)} < 5.5$ is associated with a rapid enhancement of V_L and V_R as well as with a transition to the resonant regime, which is characterized by a large current for both qubit states. Comparing Figs. 4(a) and 4(b) one can specify the region $5.5 < b_{L(R)} < 6.5$, where the measurement

conditions for the qubit are optimal for the set of other parameters indicated in the figures.

The detunings δ_L and δ_R of QD energies in the SET are obviously the main parameters of the system since their choice sets the tunneling regime and realizes the measurement principle based on the fulfillment or violation of the symmetry condition $\delta_L = \delta_R$. However, this condition in itself does not yet guarantee the large contrast and current through the SET. Figure 5 shows the dependences of the current and the contrast on the detuning in the symmetric case for three values of the distance L_y between the SET and the qubit.

It can be seen that in the resonant regime at $\delta_{L(R)} \leq 0.05$ the measurement is possible, but with less contrast than in the nonresonant one. The appearance of a wide interval, where C_I drops to zero, is associated with compensation of the energy level asymmetry in the SET for the qubit electron position in QD B due to partial recovery of resonant coupling. The active transport regardless of the qubit state is observed. In this case, the SET density matrix is in the superposition of one-, two-, and three-electron components with weights

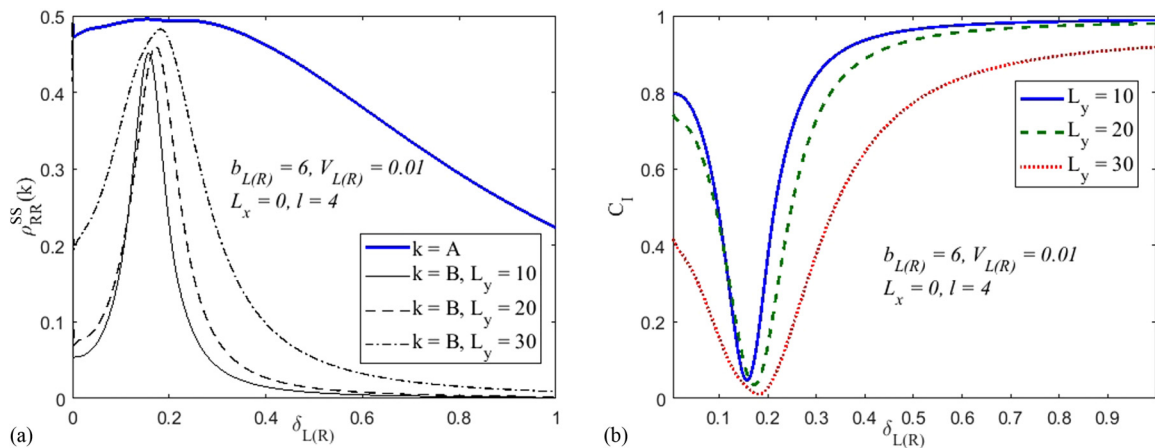


FIG. 5. Dependencies of the current (a) and the measuring contrast (b) of the SET at a symmetrical case of the detunings for three distances between the SET and the qubit. (The values are given in effective atomic units for GaAs; see text.)

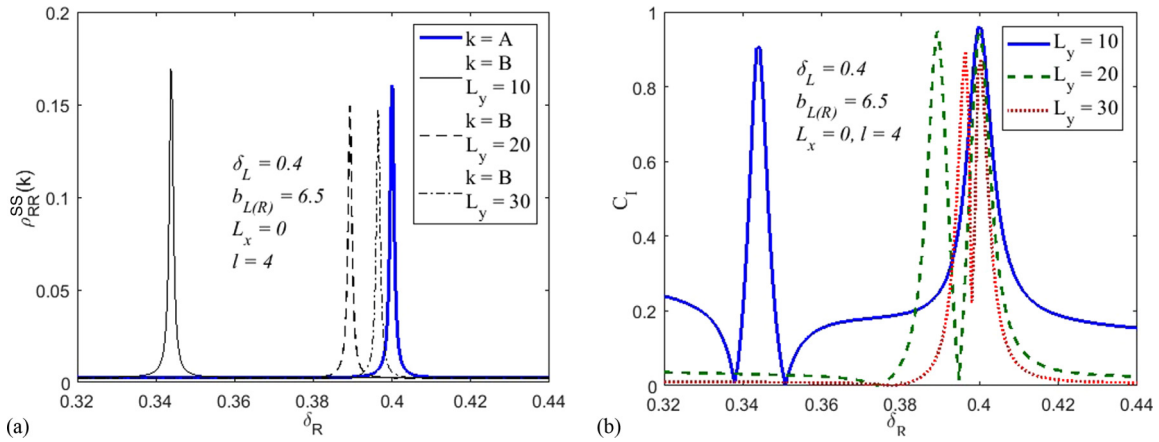


FIG. 6. The current through the SET (a) and the contrast (b) vs detuning δ_R at fixed detuning δ_L . (The values are given in effective atomic units for GaAs; see text.)

of 0.23, 0.54, and 0.23, respectively. The position and the size of this interval depend on the distance from the qubit, indicating the interplay among the Coulomb energies, the tunneling energies, the detunings, and the relaxation rates. Besides, the electron's transport from QD L into QD R under the discussed conditions is observed only at large times $t > \gamma_k^{-1}, \Gamma_{L(R)}^{-1}$ in the steady-state regime. Hence the dissipation effects (incoherent tunneling and relaxation from QD L to QD C) participate in the transport as well. The given explanation reveals the existence of specific parameter combinations for which the transport properties of SET should be treated at a more profound level. The search algorithm of those parameter combinations is to be developed in further study. The detuning choice from the interval $\delta_{L(R)} = 0.3-0.6$ guarantees simultaneously the large measured current and contrast. A further synchronous increase of detunings does not change the contrast, but for $\delta_{L(R)} > 0.6$ leads to the current suppression due to weakening of the coupling between the QDs. A drop of C_l with increasing L_y , as has been already found, is associated with vanishing of the effect of the qubit internal geometry on the current as the qubit is moved far from the SET.

Even more information can be obtained from the analysis of the current strength ρ_{RR}^{SS} and the contrast C_l for the detunings δ_L and δ_R , changing independently (Fig. 6). Let us consider the behavior of these quantities on the interval of detunings δ_R for several values δ_L and L_y . At first glance, the choice of a geometry should distinguish the symmetric case $\delta_L = \delta_R$ as the only possible one for obtaining a reasonable current through the SET, if the qubit is loaded into the state $|A\rangle$ (point $\delta_R = \delta_L = 0.4$). However, as follows from Fig. 6, there is another value $\delta'_R \neq \delta_L$ for which a large contrast is due to the presence of an electron in the qubit state $|B\rangle$. Such a change in the roles of the logical states is associated with compensating the imbalance of the detunings due to the imbalance of the energies of the Coulomb interaction of the qubit and SET electrons, $\delta'_R = \delta_L + \Delta W(L_y)$. This is confirmed by the dependence of the δ'_R position on the distance L_y and by the independence of the compensation energy $\Delta W(L_y)$ on the choice of δ_L for a fixed L_y . For the qubit located at a large distance from the SET one has $\Delta W(L_y) \rightarrow 0$ and both

peaks merge, making the measurement impossible. Recall that the presence of such special points (sweet spots), in which the symmetry is restored, is inherent in complex systems with a tunnel or optical connection between components. We also point out that the asymmetry of the tunneling energy associated with the barrier thickness difference also implies the existence of such a set of geometrical parameters for which the Coulomb energy compensates it.

The geometry of the measuring chip remains important in practical terms. As one has just seen, when the qubit is moved far from the SET the Stark QD shifts, associated with the different basis states, come closer and the measurement contrast decreases. A partial compensation for this drop is possible by increasing the linear size of the SET and the qubit, i.e., the widths of the QDs and the thicknesses of the barriers separating them. However, as shown above, varying the barrier thickness within 1–2 units of length (10–20 nm for GaAs) causes a sharp slowdown of the electron transport through the structure and the current suppression. This also applies to the DQD qubit, where fast coherent electron oscillations (quantum operations) can be realized under a sufficiently high barrier transparency that limits its thickness (and a qubit length). The use of wide QDs as well as SETs with a large number of QDs will be analyzed in further papers. As follows from Fig. 7(a), at distances of $L_y < 20$ the contrast exceeds 90%, and at $L_y > 30$ it decreases rapidly. Enhancement of the distance l between the qubit QDs A and B by one unit of length gives only a slight improvement in the contrast. Thus, there is a limitation on the measurement precision due to the finite sizes of the qubit and the SET.

The contrast also depends on the mutual orientation of the axes of the SET and the qubit [Fig. 7(b)]. If the axes are parallel to each other ($\varphi = 0$ or π), then the qubit basis states are maximally distinguishable. If they are perpendicular ($\varphi = \pi/2$ or $3\pi/2$), then, as the condition $\delta_L = \delta_R$ is now satisfied for each basis state due to the geometry, $I_A = I_B$ and $C_l = 0$. As the distance L_y increases, the areas of contrast minima become wider. In addition, one can notice a slight asymmetry of C_l with respect to the point $\varphi = \pi$, which is associated with the direction of an irreversible current flow through the SET.

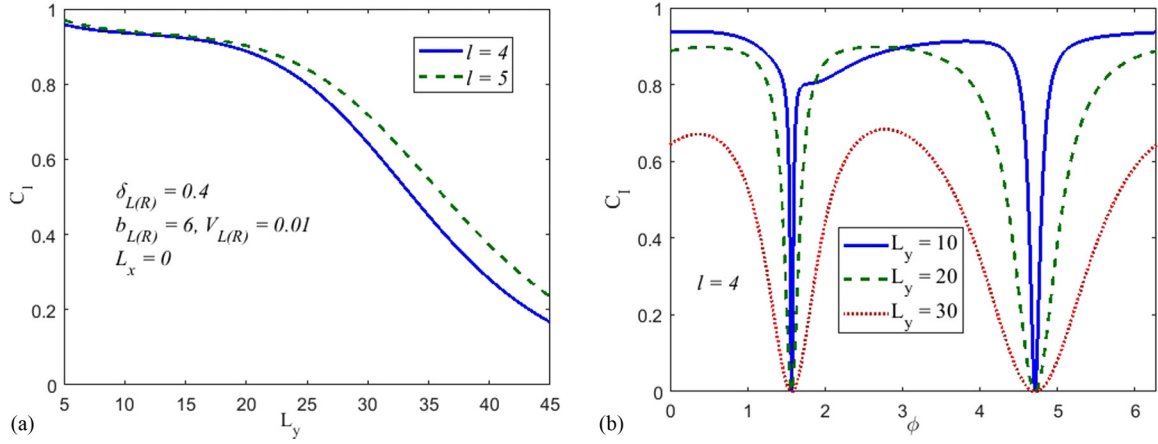


FIG. 7. The measuring contrast as functions of the distance L_y between the qubit and the SET for two qubit lengths (a) and of the angle between axes of the SET and the qubit (b). (The values are given in effective atomic units for GaAs; see text.)

The qubit in one of its logical states was considered above. Next we obtain the current through the SET for the qubit in a state with an arbitrary population distribution, when $|c_A|$ changes from 0 to 1. To get the current for high, medium, and low contrast, we choose the distance $L_y = 10, 20, 30, 40$, and 50 between the qubit and the SET. Figure 8 demonstrates the complete coincidence of the curves found by the numerical integration of Eq. (8) and by formula (12) that was derived with use of the assumption (10) about the structure of the system density matrix in the steady state. A low contrast corresponds to more smooth current dependencies for which the resolution $d\rho_{RR}^{SS}/d|c_A|$ is small. Recall that for $L_y \gg l$ this reduction is caused by a decrease in the difference of the coupling energies between the SET and the qubit being in its two logical states. In addition, at $|c_A| \ll 1$ the derivative tends to zero for any C_l value. In order to improve the measuring precision in this limit one can invert the qubit and carry out measurements in the vicinity of the point $|c_A| \approx 1$ where the derivative $d\rho_{RR}^{SS}/d|c_A|$ is maximum.

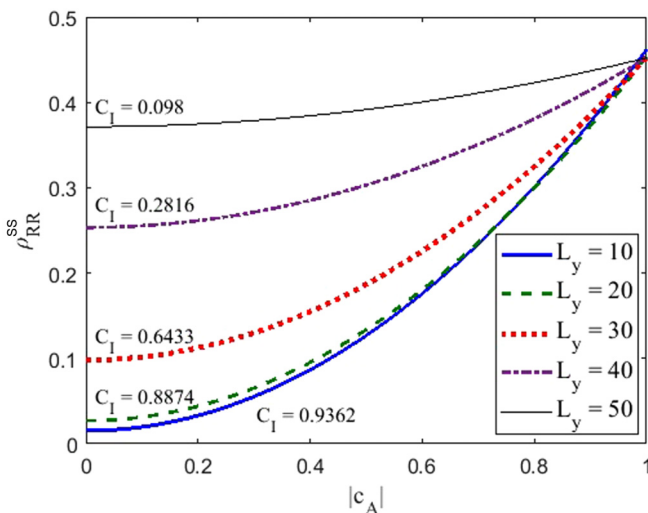


FIG. 8. The SET current vs the amplitude of the qubit basis state $|A\rangle$ for several values of the distance L_y between the SET and the qubit. (The values are given in effective atomic units for GaAs; see text.)

The sensitivity is another measure that characterizes the ability of SET to distinguish between two ultimate charge states, corresponding to the presence or absence of an electron in a single QD or to the electron position in a double QD. Following general formalism, we consider the differential conductance of the SET, $g_m = dI/dV$, to quantify the SET current change caused by qubit electron transposition between QD A and QD B [15,16]. It is easy to derive the expression for the differential conductance $g_m = C_l e(I_A + I_B)/|W_{A,R} - W_{B,R}|$ in terms of the measurement contrast, or $g_m = 2\pi\Gamma_R|\tilde{\rho}_{RR}^{SS}(A) - \tilde{\rho}_{RR}^{SS}(B)|/|W_{A,R} - W_{B,R}|$ in e^2/\hbar units. At large distances between the SET and the qubit ($L_x = 0$, $L_y \gg l$) the interaction energy difference is approximated by the expression $W_{A,R} - W_{B,R} \approx \frac{1}{L_y}(\frac{l}{L_y})^2$. Taking from Fig. 5 $\tilde{\rho}_{RR}^{SS}(A) = 0.45$ and $\tilde{\rho}_{RR}^{SS}(B) = 0.001$ at $L_y = 20$ and $\delta_{L(R)} = 0.4$ we obtain $g_m \approx 1.3 \times 10^{-2} e^2/\hbar$ and the sensitivity $5 \times 10^{-6} e/\text{Hz}^{1/2}$ [8,17]. The corresponding peak at Fig. 6 gives one the signal-to-noise ratio $S/N \approx 20$ (in Ref. [15] $S/N = 3$). The value of g_m is slightly lower (by 2.4 times) than in Ref. [15] because of the large difference in QD sizes ($a = 10$ nm in our structure and $a = 100$ nm in [15]). The sensitivities in both cases are close to each other. The further growth of g_m can be achieved by an increase of the incoherent tunneling rate Γ_R . However, this increase may stimulate cotunneling and exchange processes whose influence on the SET current was neglected here. Therefore, the SET properties optimization is to be done in further investigations.

At the end of the analysis, let us return to the qubit and show that its coupling to the SET leads to its dephasing during the time $\tau_\Gamma \sim 1/\max(\Gamma_L, \Gamma_R)$, using an equal-weighted superposition $|\Psi(0)\rangle = (|A\rangle + |B\rangle)/\sqrt{2}$ as an example. The time dependence of the off-diagonal component $\rho'_{AB}(t)$ of the qubit reduced density matrix $\rho'(t) = \text{Tr}_{\text{SET}}\rho(t)$, where the trace is now taken over the SET states, clearly illustrates the effect of dephasing (Fig. 9).

If the current does not flow through the SET, then the qubit loses coherence because of coupling to phonons. This does not affect the amplitude measurement precision; however, in order to determine the phase the Hadamard gate should be implemented as soon as possible with the aim of preserving its initial value.

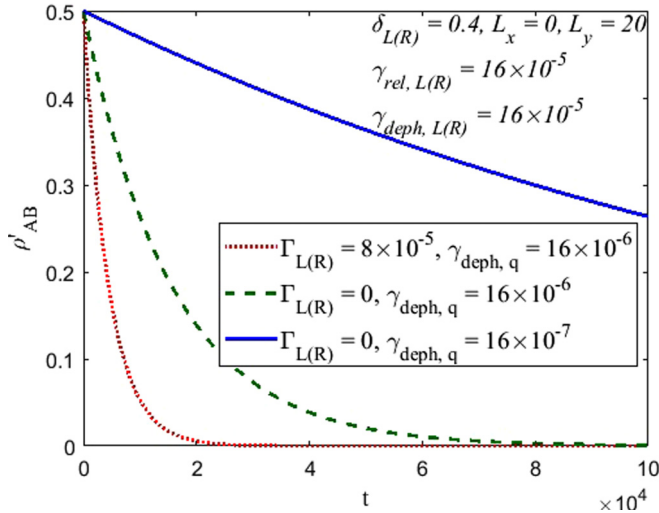


FIG. 9. The time dependence of the off-diagonal component of the qubit density matrix (coherence). (The values are given in effective atomic units for GaAs; see text.)

To compare quantitatively the efficiencies of single-QD and triple-QD SETs we note that in the resonant tunneling regime both structures demonstrate close dynamics and similar values of the measurement contrast. However, the off-resonant regime exists only for a triple-QD SET with symmetric three-level configuration. Therefore, to obtain estimations required it is suitable to compare resonant and off-resonant regimes for a triple-QD SET. As follows from Fig. 5 the contrast for the resonant regime is less than 80% whereas for the off-resonant regime it achieves values 0.99% or even higher (at 100–200 nm SET-qubit distances).

IV. DISCUSSION

In this section we briefly discuss our model in relation to other schemes of the qubit state measurement. Note that two alternative approaches to the quantum register engineering exist. The first one assumes the high level of integration where many qubits reside in the same chip [18]. All qubits are connected by a common quantum (photon, phonon, plasmon) network with the external control at single-quantum level. Usually, in that approach the single read-out device included in the network is exploited for measurement of each qubit in the register. At first glance, this design looks like a compact and economic one. However, it is easy to see that, for example, the simultaneous measurement of all qubits is impossible (perhaps except some trivial many-qubit states). Further, the quantum states of qubits placed closely to each other are spoiled by undesirable interconnections (cross talks) and, as the result, there are additional quantum errors that one needs to correct.

The second approach is based on the concept that each qubit should be supplied by its own circuitry including an individual measurement device. This design is free from the cross-talk problem and allows one to calibrate and to manipulate each qubit at an individual control level. Now one is able to measure all qubits simultaneously. As an example we mention two nitrogen-vacancy center qubits, each of them

placed in individual setups, separated by a distance of 3 m and connected by a photon network (the single-mode optical cable) [19]. Such scheme allowed the authors to obtain robust entangled states of center spins, due to cross-talk absence and fine individual center tuning and measurement. Of course, the problem of the space resource arises. However, as we expect, a compromise between compactness and robustness will be found. The scheme where the qubit is fabricated with individual control architecture (and being maximally isolated from neighboring qubits due to a wide distance) may have several advantages when compared to high-integration schemes, especially for solid-state qubits. Therefore, in view of manufacturing such qubits with closed-up control circuitry one needs, in particular, to elaborate and to optimize an individual measurement device. Our model of the triple-QD SET serves for this purpose.

Now consider other measurement techniques for comparison with the proposed scheme. One of them, namely, that with a superconducting microwave resonator, is quite popular and was successfully applied to detect an electron in a double-dot charge qubit (see, e.g., Ref. [20]). The geometric constraints related to the qubit placement in the mode antinode are much weaker than in our model. On the other hand, the semiconductor-superconductor interface requires involved technology whereas a fully semiconductor-QD chip can be fabricated in simpler way. Further, the Jaynes-Cummings electron-photon coupling that serves to monitor the charge qubit by microwave photons is weaker than Coulomb coupling between the charge qubit and an electron tunneling through the SET. This rough and brief qualitative analysis indicates the existence of advances and shortcomings inherent to each variant. Depending on technological opportunities and purposes, one can use the scheme more appropriate to date.

Meanwhile, the resonator scheme has a deeper connection to the proposed QD SET scheme. Both exploit photon or electron transport via an auxiliary object presented by a resonator or QD chain. There exists a general approach for transport property optimization that relates to the discretization of the auxiliary system spectrum. Concerning optical [21,22] or microwave [23] systems it assumes the use of a single or several active modes whereas others have to be turned off by appropriate frequency selection. This spectrum discretization in rather long systems is usually achieved by the spatial discretization of system volume: The waveguide initially presented by the continuous cable is now replaced by the resonator chain. Besides, this replacement has another consequence: The transport becomes more sensitive to the external perturbations. From a theoretical point of view both photon and electron transports are described by the widely known tunneling Hamiltonian. Even more, any QD can be treated as an “electronic resonator” confining Bloch waves in analogy with photonic resonators confining electromagnetic waves. The perturbations influence the system via detunings and tunneling energy fluctuations. In the photonics such objects are coupled resonator optical waveguides (CROWs) [21]. They are extensively studied for quantum information applications such as individual optical addressing, entangling, and measurements of solid-state qubits. In the nanoelectronics the replacement single (possibly large) island by three QDs arranged in a linear chain has the same effect on the

electron dynamics, particularly, the sensitivity growth to external charge motion in the nonresonant symmetric regime. Particularly, the high sensitivity of the spatially discretized electron transport channel (here the linear QD array or the chain) to external electrical perturbations can be explained as follows. If one operates with a small number of quantum states coupled to the neighboring states by tunneling, it is very important to conserve high coupling strengths between all pairs of neighboring states during operation. Those strengths strongly depend on the tunneling matrix elements and energy level separations (detunings). Even if the energy of only one state is shifted by some external perturbation, the transport properties of the whole chain are influenced by that local perturbation. To interrupt the transport via a large extended system with a continuous spectrum one has to substantially modify it by the energy shift of the order of the manifold bandwidth. This shift is much larger than that stopping the tunneling in the discretized analog (QD chain). In our model we vary the energy level position in the central QD (relative to energies of the outer QDs). It provides the choice of the tunneling regime (resonant or off-resonant) by the external control of the relation $V/|\delta_{L(R)}|$. As one can expect there are many ways to design the electron spectrum in the one-dimensional (1D) or two-dimensional (2D) arrays of QDs by the local QD control. Systems which are characterized by a continuous spectrum cannot be engineered in a similar way.

In this paper we consider a three-QD 1D chain whereas multi-QD 2D or even 3D complexes can be built up in layered semiconductor heterostructures. Nevertheless, the dynamical properties of the proposed structure illustrate the general principle according to which any several-electron tunnel-coupled QD system can be exploited as the highly sensitive charge sensor. Loading the SET structure in the steady-state current regime conditioned by geometric and energetic symmetry, one makes it extremely susceptible to external charge motion. The long-range character of electron-electron interactions (in contrast to the electron-photon one) as well as the fragility of nonresonant tunneling are expected to help one to detect an electron dynamics in the charge qubit. Perhaps, more sophisticated designs involving tens or even hundreds QDs will form “quantum antennas” that will be able to overcome the difficulties of several QD schemes (e.g., strong dependence of the contrast on the SET-qubit distance). Only further investigations would help one to clarify this question.

Finally, as we have already seen, the measurement schemes based on the electronic transport possess a large degree of universality. They can also be exploited to measure the single-QD spin qubit, as was described in Refs. [24,25], where an electron moves along a quantum wire in proximity of the measured QD. One of the possible optimizations of such a

scheme could be the replacement of the quantum wire by the chain of QDs as it was described in the paper for the QD charge qubit. One may expect that spin-spin interaction between the measuring and qubit electrons will also strongly depend on geometry, symmetry, and so on, that will give one additional tools to control and measure the QD spin qubit as well.

V. CONCLUSIONS

Quantum computational schemes that use information coding to electron orbital degrees of freedom in semiconductor QDs are of great interest from both experimental and theoretical points of view. The high speed of quantum operations and scalability make them very attractive for manufacturing and studying prototypes of quantum computers. In addition, a procedure for measuring a quantum state using a SET has been developed and tested. However, the conditions that ensure the reliability of quantum algorithms and measurements impose certain requirements for a chip design. For example, minimization of the Coulomb interaction of two neighboring qubits implies an increase of the distance between them, whereas it is better to choose a small distance between the SET and the qubit. Hence, each charge qubit must be equipped with an individual measuring device. The increased sensitivity of the measurements can be achieved both by the chip manufacturing technology improvement and by the search for new design solutions.

In this paper we propose to carry out measurements in the nonresonant regime of electron tunneling through the SET, consisting of three QDs. Such a three-level system, in contrast to a single-level system, provides more effective response to small changes of the electric field. The results can be applied to both electrically formed nanostructures and crystalline ones. Calculations carried out within the framework of a dynamic model, that takes into account various physical processes, indicate the possibility of high-precision qubit measurements. There are sets of parameters for which both large current and reasonable contrast are achievable at the same time. Further studies will focus on the effect of deviations of structural and dynamic parameters from symmetry on the transport properties of the SET, as well as on analyzing alternative geometries of the measuring chip.

ACKNOWLEDGMENT

The investigation was supported by Program No. 0066-2019-0005 of the Ministry of Science and Higher Education of Russia for the Valiev Institute of Physics and Technology of RAS.

-
- [1] B. A. Joyce, P. C. Kelires, A. G. Naumovets, and D. D. Vvedensky, *Quantum Dots: Fundamentals, Applications, and Frontiers*, NATO Science Series (Springer, Berlin, 2003).
 - [2] L. Fedichkin, M. Yanchenko, and K. A. Valiev, *Nanotechnology* **11**, 387 (2000).
 - [3] T. Tanamoto, *Phys. Rev. A* **61**, 022305 (2000).
 - [4] T. Hayashi, T. Fujisawa, H. D. Cheong, Y. H. Jeong, and Y. Hirayama, *Phys. Rev. Lett.* **91**, 226804 (2003).
 - [5] J. Gorman, D. G. Hasko, and D. A. Williams, *Phys. Rev. Lett.* **95**, 090502 (2005).
 - [6] J. R. Petta, A. C. Johnson, C. M. Marcus, M. P. Hanson, and A. C. Gossard, *Phys. Rev. Lett.* **93**, 186802 (2004).

- [7] M. A. Kastner, *Rev. Mod. Phys.* **64**, 849 (1992).
- [8] U. Hanke, Yu. M. Galperin, and K. A. Chao, *Appl. Phys. Lett.* **65**, 1847 (1994).
- [9] H. Brenning, S. Kafanov, T. Duty, S. Kubatkin, and P. Delsing, *J. Appl. Phys.* **100**, 114321 (2006).
- [10] V. A. Krupenin, D. E. Presnov, A. B. Zorin, and M. N. Niemeier, *J. Low Temp. Phys.* **118**, 287 (2000).
- [11] M. Kulkarni, O. Cotlet, and H. E. Türeci, *Phys. Rev. B* **90**, 125402 (2014).
- [12] E. A. Zibik, T. Grange, B. A. Carpenter, N. E. Porter, R. Ferreira, G. Bastard, D. Stehr, S. Winnerl, M. Helm, H. Y. Liu, M. S. Skolnick, and L. R. Wilson, *Nat. Mater.* **8**, 803 (2009).
- [13] A. Majumdar, M. Bajcsy, A. Rundquist, E. Kim, and J. Vučković, *Phys. Rev. B* **85**, 195301 (2012).
- [14] A. V. Tsukanov and I. Yu. Kateev, *Russ. Microelectron.* (to be published).
- [15] C. Barthel, M. Kjørgaard, J. Medford, M. Stopa, C. M. Marcus, M. P. Hanson, and A. C. Gossard, *Phys. Rev. B* **81**, 161308(R) (2010).
- [16] T. Fujita, H. Kiyama, K. Morimoto, S. Teraoka, G. Allison, A. Ludwig, A. D. Wieck, A. Oiwa, and S. Tarucha, *Phys. Rev. Lett.* **110**, 266803 (2013).
- [17] A. N. Korotkov, D. V. Averin, K. K. Likharev, and S. A. Vasenko, in *Single-Electron Tunneling and Mesoscopic Devices*, edited by H. Koch and H. Lübbig (Springer, Berlin, 1992).
- [18] H. J. Kimble, *Nature* **453**, 1023 (2008).
- [19] H. Bernien, B. Hensen, W. Pfaff, G. Koolstra, M. S. Blok, L. Robledo, T. H. Taminiau, M. Markham, D. J. Twitchen, L. Childress, and R. Hanson, *Nature* **497**, 86 (2013).
- [20] C. H. Wong and M. G. Vavilov, *Phys. Rev. A* **95**, 012325 (2017).
- [21] A. Yariv, Y. Xu, R. K. Lee, and A. Scherer, *Opt. Lett.* **24**, 711 (1999).
- [22] M. Notomi, E. Kuramochi, and T. Tanabe, *Nat. Photon.* **2**, 741 (2008).
- [23] L. Zhou, Z. R. Gong, Y.-X. Liu, C. P. Sun, and F. Nori, *Phys. Rev. Lett.* **101**, 100501 (2008).
- [24] V. Vyurkov, A. Vetrov, and A. Orlikovsky, *Proc. SPIE* **5128**, 164 (2003).
- [25] T. Otsuka, E. Abe, Y. Iye, and S. Katsumoto, *Physica E (Amsterdam, Neth.)* **42**, 809 (2010).